Synthesis, Characterization, and Morphology of Poly(*tert*-butyl vinyl ether-*b*-isobutylene-*b*-*tert*-butyl vinyl ether) Triblock Copolymers†

Yonghua Zhou and Rudolf Faust*

Polymer Science Program, Department of Chemistry, University of Massachusetts Lowell, One University Avenue, Lowell, Massachusetts 01854

Shujun Chen and Samuel P. Gido

Department of Polymer Science and Engineering, University of Massachusetts Amherst, Amherst, Massachusetts 01003

Received March 24, 2004; Revised Manuscript Received June 23, 2004

ABSTRACT: The living cationic sequential block copolymerization of isobutylene (IB) with *tert*-butyl vinyl ether (*t*BVE) was studied using a one-pot procedure in hexanes/CH_2Cl_2 and hexanes/CH_3Cl solvent systems at −80 °C. It was carried out by the so-called capping-tuning technique, involving the capping of living PIB chain ends with 1,1-ditolylethylene (DTE) followed by addition of titanium(IV) isopropoxide ($Ti(OIp)_4$) to lower the Lewis acidity before the introduction of *t*BVE. Homopolymerizations/model block copolymerizations of *t*BVE were carried out using 2-chloro-2,4,4-trimethylpentane (TMPCl) instead of living PIB. The living nature was exhibited by the linear plots of $\ln([M]_0/[M])$ vs time and number average molecular weight (M_n) vs conversion. ^{13}C NMR spectroscopy indicated that the P*t*BVE is highly isotactic with close to 80% meso dyads. Well-defined PIB-*b*-P*t*BVE diblock copolymers were synthesized by the living cationic polymerization of IB followed by capping the living PIB ends with DTE and fine-tuning the Lewis acidity to obtain 100% crossover efficiency and a desired *t*BVE polymerization rate. While both hexanes/CH_2Cl_2 and hexanes/CH_3Cl solvent systems could be used, the polymerization was better controlled and the product exhibited narrower molecular weight distribution (MWD) in hexanes/CH_3Cl solvent mixtures. Well-defined triblock copolymers with close to designed molecular weights and narrow MWDs (<1.1) were prepared using 5-*tert*-butyl-1,3-bis(1-chloro-1-methylethyl)benzene (*t*BuDiCumCl) as a difunctional initiator. Differential scanning calorimetry (DSC) of the block copolymers showed two glass transitions demonstrating microphase separation. The triblock copolymers with 23−39 wt % P*t*BVE content exhibited typical characteristics of a thermoplastic elastomer (TPE) with tensile strengths of 9−15 MPa and elongations at break of 760−1300%. Morphological studies by transmission electron microscopy (TEM), small-angle X-ray scattering (SAXS), and atomic force microscopy (AFM) revealed lamellar or cylindrical morphologies of the triblock copolymers, depending on their molecular compositions.

Introduction

Since the discovery of living cationic polymerization in the mid-1980s,[1,2] virtually all cationically polymerizable monomers have been polymerized in living cationic polymerization including isobutylene, vinyl ethers, styrene and its derivatives, and *N*-vinylcarbazole.[3−5] On the basis of these monomers, new families of pendant or terminal functional polymers, macromonomers, linear block copolymers (AB, ABA, ABC, etc.), nonlinear block copolymers (graft, star, star block, miktoarm star, etc.), and other polymers with well-defined architectures were created.

ABA triblock copolymers with polyisobutylene (PIB) as the rubbery center segment and glassy polymers as end segments, made available by living cationic polymerization, constitute a novel type of thermoplastic elastomers (TPEs), which offer improved thermal and oxidative stability over diene-based TPEs. Following the successful synthesis of poly(styrene-*b*-isobutylene-*b*-styrene),[6] various styrenic monomers such as indene,[7] *p*-methylstyrene (pMeSt),[8] and α-methylstyrene (αMeSt)[9] were used instead of styrene to incorporate polymers with higher T_g as end segments to improve the mechanical properties and upper service temperature of PIB-based TPEs.

† Polyisobutylene-Based Thermoplastic Elastomers. 8.

Recently, we have been interested in PIB-based TPEs where the end segments are polar and/or semicrystalline. While mechanistic transformations combining cationic polymerization with other living polymerization techniques have been successful to include poly(L-lactide),[10] poly(pivalolactone),[11] poly(ϵ-caprolactone),[12] poly(isobornyl acrylate),[13] and poly(methyl methacrylate)[13,14] as end segments, these transformation reactions are rather complicated. Poly(alkyl vinyl ether)s are attractive as end segments as vinyl ethers can be polymerized by living cationic polymerizations; thus poly(alkyl vinyl ether-*b*-isobutylene-*b*-alkyl vinyl ether) triblock copolymers could be prepared in a one-pot process without the complication of mechanistic transformation. These ABA triblock copolymers with high T_g end segments should be useful TPEs. Even more intriguing, however, is the opportunity that selected poly(alkyl vinyl ether)s, e.g., benzyl, trimethylsilyl, and *tert*-butyl vinyl ethers could be hydrolyzed to poly(vinyl alcohol) (PVA), a polar semicrystalline polymer. However, due to the vast difference in reactivity between vinyl ethers and isobutylene,[4] direct sequential monomer addition is not feasible for the preparation of well-defined block copolymers.[15] The living cationic polymerization of vinyl ethers requires the use of weak Lewis acids such as iodine and zinc chloride, while that of isobutylene necessitates strong Lewis acids such as titanium(IV) chloride and boron chloride. Thus, the

10.1021/ma049424u CCC: $27.50
Published on Web 08/12/2004

living poly(vinyl ether) cannot initiate the polymerization of IB, and the introduction of vinyl ethers to living PIB reaction mixtures leads to low crossover efficiency, as was the case of isobutyl vinyl ether (IBVE),[16] due to an unfavorable ratio of crossover rate over propagation rate (R_c/R_p). To increase the crossover efficiency from less reactive monomers to more reactive monomers, attempts have been made by lowering the Lewis acidity or adding common ion salts.[16,17] These attempts failed, since the decrease in R_p was inevitably accompanied by the decrease of R_c. To increase the crossover efficiency, the ratio of R_c/R_p should be increased.

In a series of publications from this laboratory,[8,18−21] a new strategy was reported for the synthesis of block copolymers by living cationic sequential block copolymerization when the second monomer is more reactive than the first one. It involves capping of PIB chain ends with 1,1-diphenylethylene (DPE) or 1,1-ditolylethylene (DTE) followed by lowering the Lewis acidity to match the reactivity of the second monomer. The purpose of the Lewis acidity tuning is to generate stronger nucleophilic counterions, which ensure a high R_c/R_p ratio, as well as the living polymerization of a second monomer. This has been carried out using three different methods: (i) by the addition of titanium(IV) alkoxide in the block copolymerization of IB with pMeSt[8,18] and methyl vinyl ether (MVE);[19] (ii) by the addition of nBu$_4$NCl in the block copolymerization of IB with isobutyl vinyl ether (IBVE);[20] (iii) by the substitution of a strong Lewis acid with a weaker one, employed in the block copolymerization of IB with αMeSt.[21] All methods succeeded in preparing pure block copolymers with 100% crossover efficiency, showing the synthetic power of the capping-tuning methodology.

Poly(*tert*-butyl vinyl ether), which has a T_g of 88 °C,[22] has long been prepared by cationic polymerization as a precursor to poly(vinyl alcohol).[23] Highly isotactic poly(vinyl alcohol), with ∼79% mm triad sequence, was derived from the poly(*t*BVE) polymerized with BF_3·OEt_2.[24] Living cationic polymerization of *t*BVE was achieved by the $CH_3CH(OiBu)OCOCH_3/Et_{1.5}AlCl_{1.5}$ initiating system in the presence of THF as "Lewis base" at −20 °C.[25] However, the polymerization was slow as close to quantitative yield was reached only in 60 h.

To the best of our knowledge, there has been no report on the synthesis of PIB based TPEs with poly(vinyl ether)s as the end segments. In this work, we report on the living cationic block copolymerization of IB with *t*BVE using the capping-tuning technique. The triblock copolymers are expected to be thermoplastic elastomers and precursors to poly(vinyl alcohol-*b*-isobutylene-*b*-vinyl alcohol).

Experimental Section

(a) Materials. *tert*-Butyl vinyl ether (*t*BVE) (98%, Aldrich) was washed with distilled water, dried over KOH overnight, and distilled from CaH_2: bp 77−78 °C. The purified *t*BVE was stored at −20 °C under nitrogen. The syntheses of 2-chloro-2,4,4-trimethylpentane (TMPCl),[26] 5-*tert*-butyl-1,3-bis(1-chloro-1-methylethyl)benzene (*t*-BuDiCumCl),[27] and ditolylethylene (DTE)[19] have been described in the literature. Titanium(IV) chloride ($TiCl_4$) (99.9%, Aldrich), 2,6-di-*tert*-butylpyridine (DTBP) (97%, Aldrich), and titanium(IV) isopropoxide (97%, Aldrich) were used as received. CH_3Cl and isobutylene (IB) were dried by passing the gas through in-line gas purifier columns packed with BaO/Drierite and condensed at −80 °C prior to polymerization. Hexanes (Hex) were rendered olefin free by refluxing over sulfuric acid (95−98%, VWR) for 48 h. It was washed first with 10% KOH aqueous solution and then with distilled water until neutral and was stored over $NaSO_4$ for at least 24 h. It was distilled before use after refluxing over CaH_2 overnight. Methylene chloride (CH_2Cl_2) was purified by washing with distilled water until neutral, drying over sodium sulfate overnight, and refluxing over P_2O_5 overnight. It was distilled twice from P_2O_5 just before use.

(b) Polymerization. All polymerizations were carried out under a dry nitrogen atmosphere in an MBraun 150-M glovebox (Innovative Technology Inc.) using hexanes (Hex)/CH_2Cl_2 or Hex/CH_3Cl solvent mixtures at −80 °C. For small reaction volumes (20−50 mL), 75- or 150-mL test tubes were used as reactors; when larger reaction volumes (100−200 mL) were desired, polymerizations were conducted in three neck round-bottomed flasks equipped with overhead stirrers. In a typical procedure for the sequential block copolymerization of IB with *t*BVE, polymerization of IB, initiated by 2-chloro-2,4,4-trimethylpentane (TMPCl) in conjunction with $TiCl_4$, was carried out for 30−60 min in the presence of 2,6-di-*tert*-butylpyridine (DTBP) as a proton trap. DTE was introduced next to cap the living PIB chain ends. After 1−2 h when capping was complete, Ti(OIp)$_4$ was added, followed by addition of *t*BVE 5 min thereafter. Finally, the reactions were quenched with prechilled methanol at predetermined time intervals. The reaction mixtures were poured into excess 10% ammoniacal methanol and dried under the hood. The polymer was dissolved in Hex, filtered, purified twice by dissolution in Hex and precipitation in methanol, and then dried in vacuo for 24 h. In homopolymerization of *t*BVE, TMPCl was directly capped with DTE, followed by introduction of Ti(OIp)$_4$ and *t*BVE. In syntheses of triblock copolymers, *tert*-butyl-1,3-bis-(1-chloro-1-methylethyl)-benzene (*t*BuDiCumCl) was used as the initiator instead of TMPCl.

Homopolymerization of *t*BVE. In a typical experiment the polymerization was carried out in Hex/CH_3Cl (60/40, v/v) at −80 °C using the following concentrations: [TMPCl] = 0.002 M; [DTBP] = 0.004 M; [$TiCl_4$] = 0.036 M; [DTE] = 0.004 M; [Ti(OIp)$_4$]/[$TiCl_4$] = 1.6; [*t*BVE] = 0.838 M. Into a 75 mL culture tube immersed in heptane at −80 °C were added 11.35 mL of Hex at room temperature, 7.63 mL of CH_3Cl at −80 °C, 0.45 mL of DTBP stock solution in Hex at −80 °C (0.178 M), 0.89 mL of TMPCl stock solution in Hex at −80 °C (0.045 M), and 1 mL of $TiCl_4$ stock solution in Hex/CH_3Cl (60/40, v/v) at −80 °C (0.72 M). About 10 min later 1 mL of DTE stock solution in Hex/CH_3Cl (60/40, v/v) at −80 °C (0.08 M) was added, and the light yellow color of the reaction mixture turned crimson as the capping reaction proceeded. After 1 h, 4.25 mL of Ti(OIp)$_4$ stock solution in Hex/CH_3Cl (60/40, v/v) at −80 °C (0.271 M) was charged into the culture tube. In a couple of minutes, the crimson color faded and a pale green color developed. After a few more minutes 2.2 mL of *t*BVE at room temperature was added. The solution turned colorless in 1 min. The polymerization was quenched 20 min later with 2 mL of prechilled methanol at −80 °C. After purification and drying in vacuo, the polymer weighed 1.57 g (monomer conversion: 93.7%; M_n = 42.7 kg/mol; M_w/M_n = 1.05).

Synthesis of P*t*BVE-*b*-PIB-*b*-P*t*BVE Triblock Copolymers. In a typical experiment the polymerization was carried out in Hex/CH_3Cl (60/40, v/v) at −80 °C using the following concentrations: [*t*BuDiCumCl] = 0.001 M; [DTBP] = 0.004 M; [$TiCl_4$] = 0.036 M; [IB] = 1.25 M; [DTE] = 0.004 M; [$Ti(OIp)_4$]/[$TiCl_4$] = 1.6; [*t*BVE] = 0.4 M. Into a 500 mL round-bottom flask immersed in heptane at −80 °C were added 105.5 mL of Hex at room temperature, 62.1 mL of CH_3Cl at −80 °C, 8.9 mL of DTBP stock solution in Hex at −80 °C (0.089 M), 10 mL of *t*BuDiCumCl stock solution in Hex at −80 °C (0.02 M), and 10 mL of $TiCl_4$ stock solution in Hex/CH_3Cl (60/40, v/v) at −80 °C (0.72 M). About 10 min later 19.4 mL of IB at −80 °C was added and polymerized for 2 h. At the end of polymerization of IB was added 10 mL of DTE stock solution in Hex/CH_3Cl (60/40, v/v) at −80 °C (0.08 M). After 1 h, 42.5 mL of $Ti(OIp)_4$ stock solution in Hex/CH_3Cl (60/40, v/v) at −80 °C (0.271 M) was charged into the flask. After ∼2 min, 1 mL of the reaction mixture was taken from the flask and quenched with 2 mL of prechilled methanol for molecular weight measurement of the PIB middle segment (M_n = 69.4 kg/mol; M_w/M_n = 1.08). After ∼3 min 10.5 mL of *t*BVE at room temperature was added. After 3 h, 10 mL of prechilled methanol was charged into the flask. After purification and drying in vacuo, the triblock copolymer weighed 21.54 g (overall monomer conversion: 98%; M_n = 110.6 kg/mol; M_w/M_n = 1.08).

(c) Molecular Characterization. NMR spectroscopy was carried out on a Bruker 250 or 500 MHz instrument. Scanning visible spectroscopic analysis was performed with a model 661.300 all quartz immersion probe connected to a LS-1 fiber optic tungsten light source (Ocean Optics) and a Zeiss MMS photodiode array detector. The entire system was driven by a Tec 5 interface and Aspect Plus software (Zeiss).

Molecular weights were measured with a size-exclusion chromatography system consisting of a model 510 HPLC pump, a model 486 tunable UV/visible detector (Waters) with a wavelength tuned at 254 nm, a model 250 RI/viscosity detector (Viscotek) equipped with a 670 nm light source, and five Ultrastyragel GPC columns connected in the following series: 500, 10^3, 10^4, 10^5, and 100 Å. Samples were eluted in THF at a flow rate of 1 mL/min and analyzed using Viscotek version 3.0 universal and conventional calibration software. Refractive index increments (d*n*/d*c*) used for absolute molecular weight determinations were calculated from the individual d*n*/d*c* values of PIB (0.11 mL/g) and P*t*BVE (0.0637 mL/g), as determined by a laser interferometer (Optilab, Wyatt Technology Inc.) operating at λ = 690 nm in THF, based on their relative composition.

The glass transition temperatures (T_gs) of the triblock copolymers were determined by a DuPont 910 differential scanning calorimeter calibrated with indium for onset temperature and enthalpy change. The T_g was determined as the temperature where the heat flow curve reached the half step-height (plotted by extrapolation of the linear range below and above the glass transition). The samples were heated to 150 °C at 20 °C/min, held isothermal for 5 min and then cooled to −110 °C at 20 °C/min. Thermograms were recorded during the second heating cycle from −110 to 150 °C at 20 °C/min. The tensile properties were measured on compression-molded samples according to ASTM D412.

(d) Morphological Characterization. Solid films approximately 1 mm thick of the triblock copolymers were slowly cast from 5 wt % polymer solutions in toluene, a nonpreferential solvent. Casting was performed at room temperature, and the evaporation of solvent was controlled to form a solid film after 7−10 days. The films were given another 1 week under high vacuum at room temperature to remove residual solvent. The samples were then annealed for 1 week under high vacuum at 100 °C to further promote the approach to an equilibrium structure.

After annealing, samples for electron microscopy were cryomicrotomed in a Leica ultramicrotome. Sections approximately 40−60 nm thick were cut with a Diatome diamond knife at a sample temperature of −85 °C and a knife temperature of −85 °C. The sections were stained in RuO_4 vapor for about 4 h. Transmission electron microscopy (TEM) was performed on a JEOL 2000FX transmission electron microscope operated at 200 kV accelerating voltage.

Small-angle X-ray scattering (SAXS) experiments were performed on annealed films using a Molecular Metrology 2D SAXS instrument powered by a high-brilliance Osmic Max-Flux source with Cu Kα sealed-tube X-ray radiation and pinhole collimation. Patterns were collected digitally with a 2D multiwire detector and analyzed with a FAST ComTec MPA-3 multichannel analyzer and custom-written software. Extraneous background scatter was subtracted, and the data were plotted on a logarithmic scale. Circular averaging was performed to produce a plot of intensity vs scattering angle, q.

In addition, atomic force microscopy (AFM) experiments were done on unannealed films of the triblock copolymers spin coated on Si wafers, with a Digital Instruments D3100 scanning force microscope in the tapping mode. To be consistent with TEM and SAXS experiments, 5 wt % toluene solutions were used for the spin coating of the triblock copolymers, resulting in a polymer film thickness of about 200 nm.

Results and Discussion

(a) Homopolymerization of *t*BVE and Block Copolymerization of IB with *t*BVE in Hex/CH_2Cl_2 Solvent Mixtures. Experimentation started with a similar procedure found successful in the synthesis of PIB-PMVE block copolymers[19,28] (Hex/CH_2Cl_2 = 50/50 v/v; [DTBP] = 0.006 M; [$TiCl_4$] = 0.064 M; [TMPCl] = 0.004 M; [DTE] = 0.008 M; [$Ti(OIp)_4$]/[$TiCl_4$] = 0.7; [*t*BVE] = 0.339 M). Thus, DTE was used as the capping agent instead of DPE,[19] and *t*BVE was introduced within 5 min after addition of $Ti(OIp)_4$ to minimize decapping.[28] The color of the reaction mixture turned orange after the introduction of DTE, and a chocolate brown color developed after the addition of $Ti(OIp)_4$. It was found that the polymerization of *t*BVE was completed in less than 2 min at −80 °C, while under similar conditions the polymerization of MVE was slow and incomplete. This is in accord with earlier findings that *t*BVE is much more reactive than MVE in cationic polymerizations.[29] More importantly, however, complexation of Lewis acid with PMVE, which necessitated the temperature increase to 0 °C to shift the equilibrium of complex formation toward free Lewis acid,[30] is unlikely with P*t*BVE due to the bulky *tert*-butyl group. Due to these considerations at [$Ti(OIp)_4$]/[$TiCl_4$] = 0.7 the polymerization of *t*BVE was very fast and the homo-

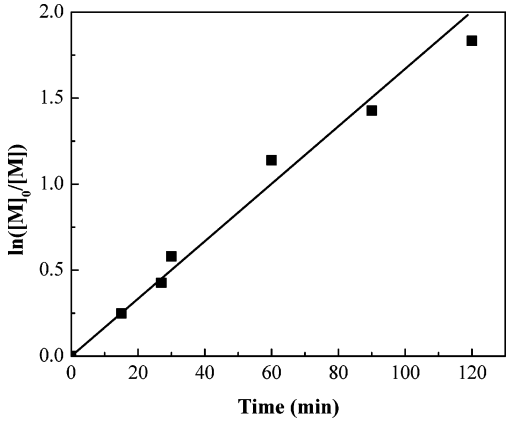

Figure 1. ln([M]$_0$/[M])−time plot for homopolymerization of *t*BVE. Reaction conditions: [TMPCl] = 0.002 M; [$TiCl_4$] = 0.036 M; [DTBP] = 0.004 M; [DTE] = 0.004 M; Ti(OIp)$_4$/[$TiCl_4$] = 2.0; [*t*BVE] = 0.762 M in Hex/CH_2Cl_2 (60/40, v/v) at −80 °C.

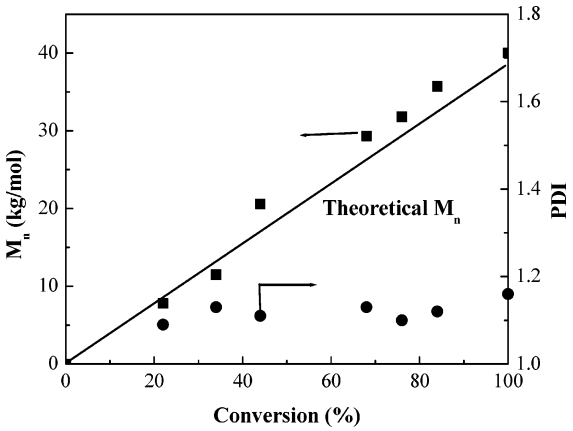

Figure 2. M_n−conversion plot for polymerization of *t*BVE. For reaction conditions, see Figure 1.

polymer exhibited broad molecular weight distribution (MWD). Apparently for *t*BVE a higher ratio of [Ti(OIp)$_4$]/[$TiCl_4$] should be used to effect control of living polymerization.

Kinetics and Livingness of Homopolymerization of *t*BVE. When an increased [Ti(OIp)$_4$]/[$TiCl_4$] ratio of 2.0 was used, 100% conversion was attained in 4 h after addition of *t*BVE, and the homopolymerization exhibited a living character. The livingness of polymerization is shown by the diagnostic linear plots of ln([M]$_0$/[M]) vs time (Figure 1) and M_n vs conversion (Figure 2). The evolution of GPC traces with conversion is shown in Figure 3.

Block Copolymerization of IB with *t*BVE. Diblock copolymerization was carried out in Hex/CH_2Cl_2 = 60/40 v/v at −80 °C using [Ti(OIp)$_4$]/[$TiCl_4$] ratios varied over the range of 1.0−2.4 under the following conditions: [TMPCl] = 0.002 M; [IB] = 0.1 M; [$TiCl_4$] = 0.036 M; [DTBP] = 0.004 M; [DTE] = 0.004 M; [*t*BVE] = 0.191 M. All samples were quenched 2 h after the addition of *t*BVE. Chain end analysis by ^{1}H NMR spectroscopy indicated that the capping reaction is quantitative in 1 h, as shown by the disappearance of peaks (∼1.7 and ∼2.0 ppm) due to chlorine ended PIB and appearance of peaks (∼2.3, ∼2.5, and ∼3.0 ppm) due to DTE-capped PIB (Figure 4, spectra I and II).[19] The capping and tuning processes in the block copolymerization were

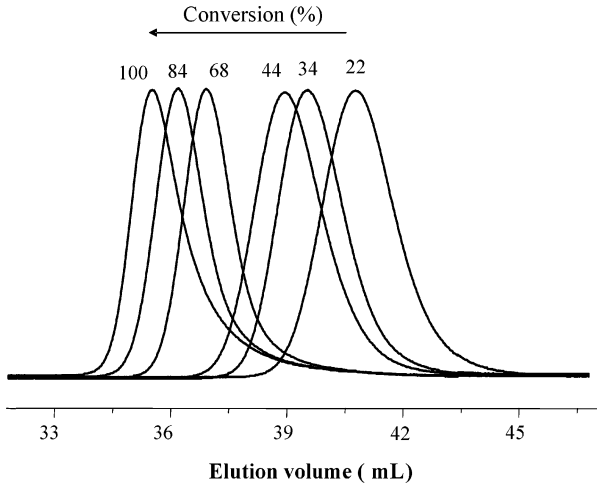

Figure 3. GPC RI traces of P*t*BVE at different conversions of *t*BVE. For reaction conditions, see Figure 1.

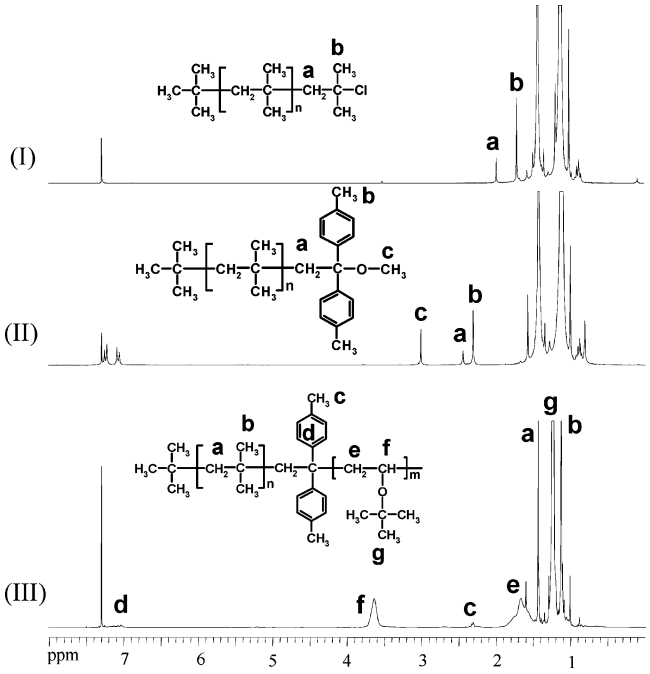

Figure 4. ^{1}H NMR spectra of samples quenched with methanol: (I) PIB before capping; (II) DTE-capped PIB; (III) PIB-DTE-P*t*BVE diblock copolymer.

studied by UV−visible spectroscopy. The bis(4-methylphenyl)carbenium ion (PIB-DTE$^+$) showed an absorption maximum at λ_{max} = 466 nm, which is almost identical with that reported for the DTE-capped dimeric IB end (λ_{max} = 464 nm in Hex/MeCl (60/40, v/v))[31] or for the DTE-capped dimeric styrene end (λ_{max} = 467 nm in $CHCl_3/CH_2Cl_2$ (70/30, v/v)).[32] As shown in Figure 5 the capping reaction was completed in ∼30 min. From the maximum absorption at the plateau [PIB-DTE$^+$] = 0.002 M was calculated; i.e., all chain ends were capped. Upon addition of Ti(OIp)$_4$, the concentration of PIB-DTE$^+$ decreased dramatically, to an undetectable level. This indicated that extent of ionization greatly decreased with the decrease of Lewis acidity, since chain end analysis by ^{1}H NMR spectroscopy showed that all PIB chain ends were still capped with DTE.

On the basis of the study by UV−visible spectroscopy, the scheme for the block copolymerization is shown in Scheme 1.

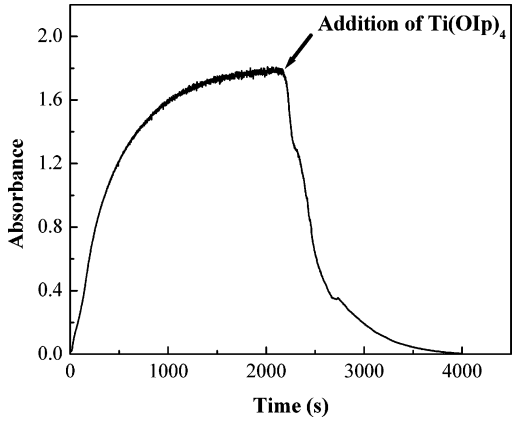

Figure 5. Plot of the absorbance at $\lambda = 466$ nm vs time for the capping reaction of living PIB ($M_n = 2{,}600$ g/mol; $M_w/M_n = 1.11$) with DTE followed by tuning of Lewis acidity with $Ti(OIp)_4$. Reaction conditions: [PIB] = 0.002 M; [$TiCl_4$] = 0.036 M; [DTBP] = 0.004 M; [DTE] = 0.004 M; [$Ti(OIp)_4$]/[$TiCl_4$] = 2.0 in Hex/CH_2Cl_2 (60/40, v/v) at −80 °C.

Structural analysis of the block copolymers by ^{1}H NMR spectroscopy indicated that 100% crossover efficiency was obtained at all [$Ti(OIp)_4$]/[$TiCl_4$] ratios as DTE-capped homo-PIB was absent (Figure 4, spectrum III). When the crossover was incomplete, the DTE-capped homo-PIB could be detected by ^{1}H NMR spectroscopy.[33] The absence of PIB-Cl peaks at ∼1.7 and ∼2.0 ppm (Figure 4, spectrum III) suggested that decapping did not occur even at [$Ti(OIp)_4$]/[$TiCl_4$] = 2.4, which was collaborated by the smooth shift of GPC traces from that of the starting PIB (Figure 6). For [$Ti(OIp)_4$]/[$TiCl_4$] = 1.0 and 1.3 the block copolymers exhibited broad/multimodal MWDs (Figure 6). At [$Ti(OIp)_4$]/[$TiCl_4$] ≥ 1.8, unimodal and relatively narrow distributions were obtained (Figure 6). With increasing [$Ti(OIp)_4$]/[$TiCl_4$] ratio the polymerization rates (as indicated by the *t*BVE conversions) and the M_w/M_n values slightly decreased (Table 1).

Synthesis of Triblock Copolymers. Triblock copolymers were synthesized using *t*BuDiCumCl as the difunctional initiator and a ratio of [$Ti(OIp)_4$]/[$TiCl_4$] = 2.0. As shown in Figure 7, the triblock copolymer exhibited close to theoretical molecular weight and relatively narrow MWD.

(b) Homopolymerization of *t*BVE Block Copolymerization of IB with *t*BVE in Hex/CH_3Cl Solvent Mixtures. The use of CH_2Cl_2 was necessary in the block copolymerization of IB with MVE because of the need to carry out polymerizations at 0 °C.[19] Since the polymerization of *t*BVE proceeds rapidly even at −80 °C, experiments were subsequently conducted in Hex/MeCl solvent mixtures. The advantages of MeCl over CH_2Cl_2 were ease of purification and, more importantly, better control over polymerization.

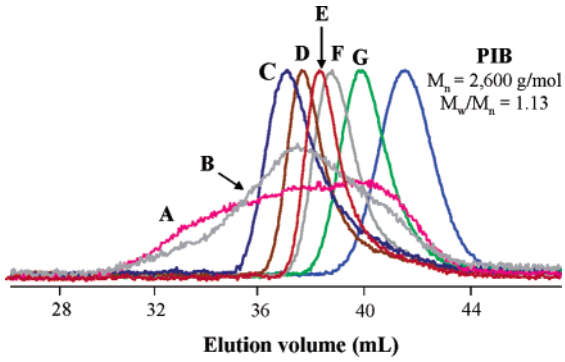

Figure 6. GPC RI traces of starting PIB and PIB-*b*-P*t*BVE block copolymers synthesized at different [$Ti(OIp)_4$]/[$TiCl_4$] ratios (A, 1.0; B, 1.3; C, 1.6; D, 1.8; E, 2.0; F, 2.2; G, 2.4). For reaction conditions, see Table 1.

Table 1. Effect of [$Ti(OIp)_4$]/[$TiCl_4$] on Block Copolymerization[a]

sample	[$Ti(OIp)_4$]/[$TiCl_4$]	conversn of *t*BVE (%)	crossover efficiency (%)	M_w/M_n
A	1.0	100	100	4.19
B	1.3	100	100	2.80
C	1.6	100	100	1.45
D	1.8	81	100	1.28
E	2.0	64	100	1.23
F	2.2	47	100	1.21
G	2.4	22	100	1.14

[a] Reaction conditions: [TMPCl] = 0.002 M; [$TiCl_4$] = 0.036 M; [DTBP] = 0.004 M; [IB] = 0.1 M; [DTE] = 0.004 M; [*t*BVE] = 0.191 M in Hex/CH_2Cl_2 (60/40, v/v) at −80 °C; all samples quenched 2 h after addition of *t*BVE.

Kinetics and Livingness of Homopolymerization. Using a [$Ti(OIp)_4$]/[$TiCl_4$] ratio of 1.6 the polymerization was completed in 40 min. The linear first-order $\ln([M]_0/[M])$ vs time plot starting at the origin (Figure 8) and the linear M_n vs conversion plot close to the theoretical line (Figure 9) indicated that the polymerization proceeds without chain transfer and termination. The evolution of GPC traces, shown in Figure 10, also confirmed the living nature of homopolymerization.

The triad tacticity of the P*t*BVE was determined by ^{13}C NMR spectroscopy according to the literature.[34,35]

Scheme 1. Capping-Tuning Process for Block Copolymerization of IB with *t*BVE

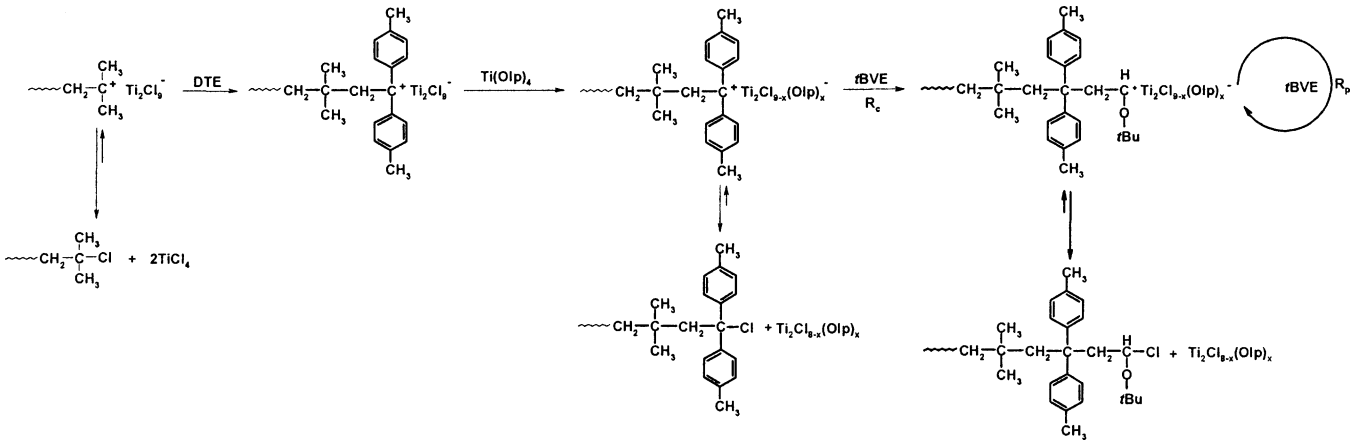

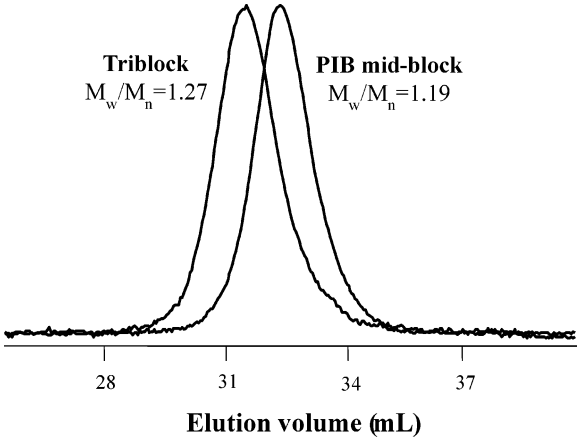

Figure 7. GPC RI traces of P*t*BVE-*b*-PIB-*b*-P*t*BVE triblock copolymer (molecular weight 16 700−65 200−16 700) and starting PIB midblock. Reaction conditions: [*t*BuDiCumCl] = 0.001 M; [$TiCl_4$] = 0.036 M; [DTBP] = 0.004 M; [DTE] = 0.004 M; [*t*BVE] = 0.314 M in Hex/CH_2Cl_2 (60/40, v/v) at −80 °C; *t*BVE polymerized for 6 h.

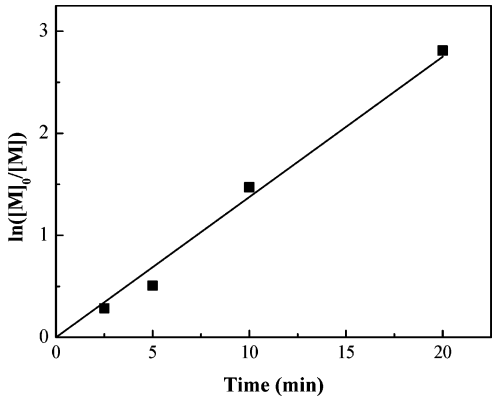

Figure 8. $\ln([M]_0/[M])$−time plot for the polymerization of *t*BVE. Reaction conditions: [TMPCl] = 0.002 M; [$TiCl_4$] = 0.036 M; [DTBP] = 0.004 M; [DTE] = 0.004 M; [*t*BVE] = 0.838 M in Hex/CH_3Cl (60/40, v/v) at −80 °C.

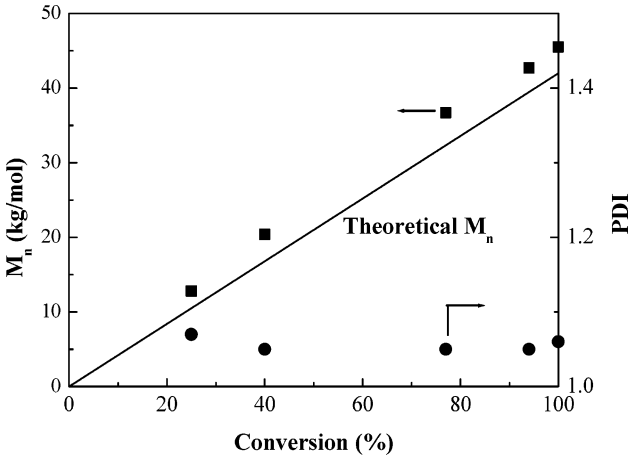

Figure 9. M_n−conversion plot for polymerization of *t*BVE. For reaction conditions, see Figure 8.

For better resolution, a high temperature of 90 °C was used. As shown in Figure 11, the P*t*BVE has 62% triad and 80% dyad isotacticity. To date, the highest isotacticity of P*t*BVE (mm = ∼79%) was obtained by conventional cationic polymerization,[24] but there has been no other report on highly isotactic P*t*BVE by living polymerization. As the effects on tacticity are many, including monomer, Lewis acid, solvent, and temperature, etc.,[36]

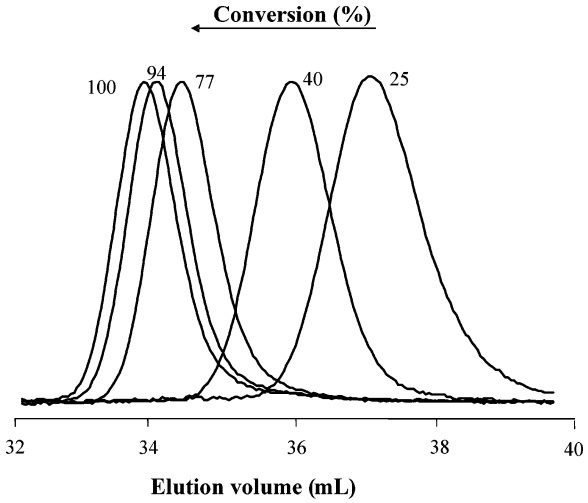

Figure 10. GPC RI traces of P*t*BVE at different conversions of *t*BVE. For reaction conditions, see Figure 8.

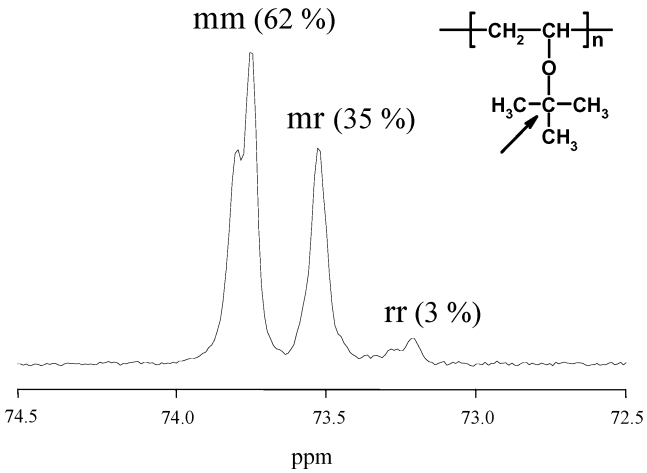

Figure 11. ^{13}C NMR spectrum (500 MHz, toluene-d_8, 90 °C) of P*t*BVE around 72.5−74.5 ppm.

Table 2. Effect of [$Ti(OIp)_4$]/[$TiCl_4$] on Block Copolymerization[a]

sample	[$Ti(OIp)_4$]/[$TiCl_4$]	conversn of *t*BVE (%)	crossover efficiency (%)	M_w/M_n
A	1.4	100	100	1.06
B	1.6	100	100	1.07
C	1.7	86	100	1.04
D	1.8	77	100	1.03
E	1.9	62	100	1.04
F	2.0	33	100	1.10
G	2.2	11	100	1.09

[a] Reaction conditions: [TMPCl] = 0.002 M; [$TiCl_4$] = 0.036 M; [DTBP] = 0.004 M; [IB] = 0.1 M; [DTE] = 0.004 M; [*t*BVE] = 0.381 M in Hex/CH_3Cl (60/40, v/v) at −80 °C; all samples quenched 2 h after addition of *t*BVE.

the mechanism of stereoregulation cannot be discussed in this paper.

Block Copolymerization of IB with *t*BVE. Since the optimum [$Ti(OIp)_4$]/[$TiCl_4$] ratio is expected to change with solvent polarity, the effect of [$Ti(OIp)_4$]/[$TiCl_4$] ratio on the polymerization rate and MWDs was studied. The results are shown in Table 2. Similar to the results with Hex/CH_2Cl_2 solvent mixtures, 100% crossover efficiency was obtained for all the samples as determined by chain end analysis, and the polymerization rate of *t*BVE decreased with increasing [$Ti(OIp)_4$]/[$TiCl_4$] ratio as suggested by the decrease of conversion.

Table 3. Samples of Triblock Copolymers

	PIB		triblock		size of P*t*BVE	P*t*BVE content (NMR)			P*t*BVE content (calcd from feed)		
no.	$10^{-3}M_n$	M_w/M_n	$10^{-3}M_n$	M_w/M_n	segments	mol %	wt %	vol[a] %	mol %	wt %	vol[a] %
A	69.4	1.08	110.5	1.08	2 × 20 600	27	39	38	25	37	36
B	66.6	1.07	96.4	1.07	2 × 14 900	21	33	32	20	31	30
C	67.3	1.06	85.9	1.08	2 × 9300	15	23	22	13	22	21

[a] Volume fractions were calculated using the following densities: $d_{PtBVE} = 0.957$ g/cm^3 and $d_{PIB} = 0.915$ g/cm^3.

Table 4. Tensile Properties of Triblock Copolymers

no.	100% modulus (MPa)	200% modulus (MPa)	300% modulus (MPa)	400% modulus (MPa)	500% modulus (MPa)	tensile strength (MPa)	elongatn at break (%)
A	2.34	2.93	4.31	5.65	7.24	12.52	760
B	1.59	1.97	2.94	4.32	6.08	15.11	800
C	0.90	1.18	1.38	1.46	1.93	9.16	1300

However, very narrow MWD ($M_w/M_n < 1.1$) was obtained even at $[Ti(OIp)_4]/[TiCl_4] = 1.4$, in sharp contrast to the broad MWD at low $[Ti(OIp)_4]/[TiCl_4]$ ratios in the Hex/CH_2Cl_2 solvent system. The GPC traces of all samples are shown in Figure 12. The better control of polymerization in the Hex/MeCl was probably due to a much faster exchange rate between the dormant and active species. Thus, well-defined block copolymers can be prepared in a wide range of $[Ti(OIp)_4]/[TiCl_4]$ ratios while achieving high conversions in a short time.

Synthesis of Triblock Copolymers. A series of P*t*BVE-PIB-P*t*BVE triblock copolymers with approximately constant PIB molecular weight and different compositions were synthesized with a $[Ti(OIp)_4]/[TiCl_4]$ ratio of 1.6. The GPC traces of a representative triblock copolymer and the PIB precursor are shown in Figure 13. The M_ns, MWDs, and compositions are summarized in Table 3. The experimental and theoretical M_ns were very close, and the narrow MWDs of the products suggest that well-defined triblock copolymer were obtained. The composition of the triblock copolymers, as calculated by ^{1}H NMR spectroscopy, agreed well with the feed composition, indicating the complete conversions of both IB and *t*BVE. The volume fractions of the P*t*BVE blocks were calculated on the basis of the measured density of P*t*BVE, 0.957 g/cm^3, and known density of PIB.[37] The density of P*t*BVE was measured using the displacement method by submerging a compression-molded sample of P*t*BVE homopolymer into *n*-butanol, a nonsolvent, according to ASTM D792.

Thermal Transitions. A DSC scan of a representative triblock copolymer (sample A) is shown in Figure 14. The two glass transitions at ~−64 °C (T_g of PIB) and ~74 °C (T_g of P*t*BVE) clearly indicate microphase separation.

Mechanical Properties. The tensile properties of the triblock copolymers have been determined, and the results are summarized in Table 4. The TPE characteristics are shown by the tensile strengths of 9−15 MPa and elongations at break of 760−1300%. At low strains (<500%), the modulus increased with increasing P*t*BVE content. Compared to PSt-PIB-PSt of similar compositions, the tensile strength of P*t*BVE-PIB-P*t*BVE is somewhat lower and the ultimate elongation higher.

Morphology. The results from the morphological characterization confirm the microphase separation behavior of the triblock copolymers. More specifically, samples A and B, with 0.38 and 0.32 combined volume fractions for the two P*t*BVE blocks, respectively, yield lamellar morphologies. Sample C, with a combined volume fraction of 0.22 for the two P*t*BVE blocks, yields a cylindrical morphology.

Shown in Figure 15 are three representative TEM micrographs of the triblock copolymers, in all of which the dark phase is P*t*BVE and the light phase is PIB, due to the selective staining of P*t*BVE blocks by RuO_4. RuO_4 has been known to be a good staining agent for poly(methyl vinyl ether) (PMVE),[38] but its staining effect on P*t*BVE has not yet been reported. Our experimental results showed that RuO_4 could selectively stain the P*t*BVE blocks in the triblock copolymers, but the staining time was much longer, about 4 h, than that needed to stain PMVE, about 15 min.[38]

Figure 15a shows a well-ordered area of lamellae in sample A, with an apparent lamellar long period (L) of 17 nm. The area shown comes from a lamellar grain of larger than 1 μ × 1 μ in size, demonstrating the good long-range order in this sample. Figure 15b shows several grains of lamellae in sample B, including an Ω tilt grain boundary defect[39] in the upper left corner of the TEM micrograph. The volume fraction of sample B, 0.32, falls in the volume fraction range where cylindrical morphology would normally be expected. The presence of the Ω tilt grain boundary, which is a common defect among lamellar grains, supports the assignment of a lamellar morphology to sample B. The apparent lamellar long period (L) of sample B is 16 nm. In both parts a and b of Figure 15 the light PIB layers look narrower than the volume fractions of PIB (0.62 and 0.68, respectively) would suggest. This is probably due to the shrinkage of the PIB layers in the electron beam during TEM observation, since PIB is a known beam-sensitive material. Figure 15c shows a poorly ordered cylindrical morphology in sample C. In the top center of the image, the projection is approximately down the cylinder axis, while on both sides of the image the projection is approximately perpendicular to the cylinder axis. This TEM image indicates a d_{10} spacing of about 21 nm. Here, again the dark P*t*BVE cylinders look larger than the 0.22 volume fraction of P*t*BVE would suggest, most likely due to the shrinkage of PIB matrix in the electron beam.

SAXS patterns of the triblock copolymers are shown in Figure 16. Figure 16a shows the SAXS pattern of sample A, having three observable reflections with ratios q_n/q^*, of the nth reflection scattering vector to the first reflection scattering vector, of 2, 3, and 4. In this figure, the 1st order reflection is very weak, but the ratios of the other, stronger peaks and the comparison to TEM data support our lamellar morphological assignment and the peak assignment given in the figure. Figure 16b shows the SAXS pattern of sample B, with two strong reflections, corresponding to its 3rd and 4th order X-ray reflections, as well as a shoulder, corre-

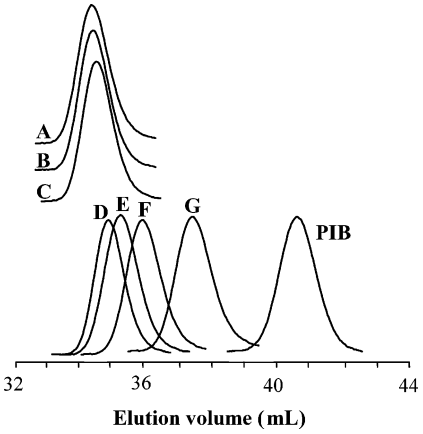

Figure 12. GPC RI traces of PIB and block copolymers synthesized at different $[Ti(OIp)_4]/[TiCl_4]$ ratios (A, 1.4; B, 1.6; C, 1.7; D, 1.8; E, 1.9; F, 2.0; G, 2.2). For reaction conditions, see Table 2.

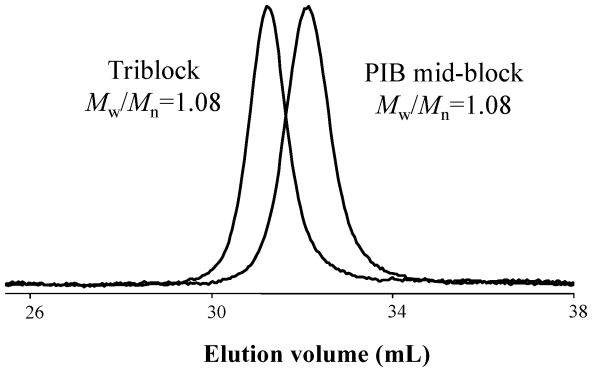

Figure 13. GPC RI traces of P*t*BVE-*b*-PIB-*b*-P*t*BVE triblock copolymer (molecular weight 20 600−69 400−20 600) and starting PIB midblock. Reaction conditions: [*t*BuDiCumCl] = 0.001 M; $[TiCl_4]$ = 0.036 M; [DTBP] = 0.004 M; [DTE] = 0.004 M; [*t*BVE] = 0.419 M in Hex/CH_3Cl (60/40, v/v) at −80 °C; *t*BVE polymerized for 3 h.

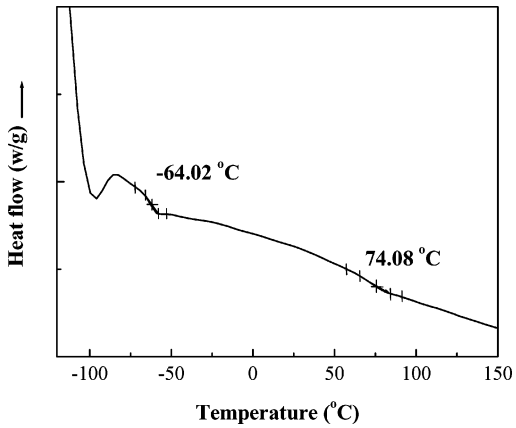

Figure 14. DSC scan of a representative P*t*BVE-*b*-PIB-*b*-P*t*BVE triblock copolymer (molecular weight 20 600−69 400−20 600).

sponding to the 1st order reflection. The presence of reflection ratios of 1, 3, and 4 further confirms the lamellar morphology of sample B. The lamellar long periods (L) of samples A and B, on the basis of the q^* values in SAXS, are 39 and 38 nm, respectively. These values are much larger than those obtained from TEM. This may also be attributed to the beam shrinkage of PIB layers during TEM observation. This conclusion is supported by AFM images on thin films, not shown,

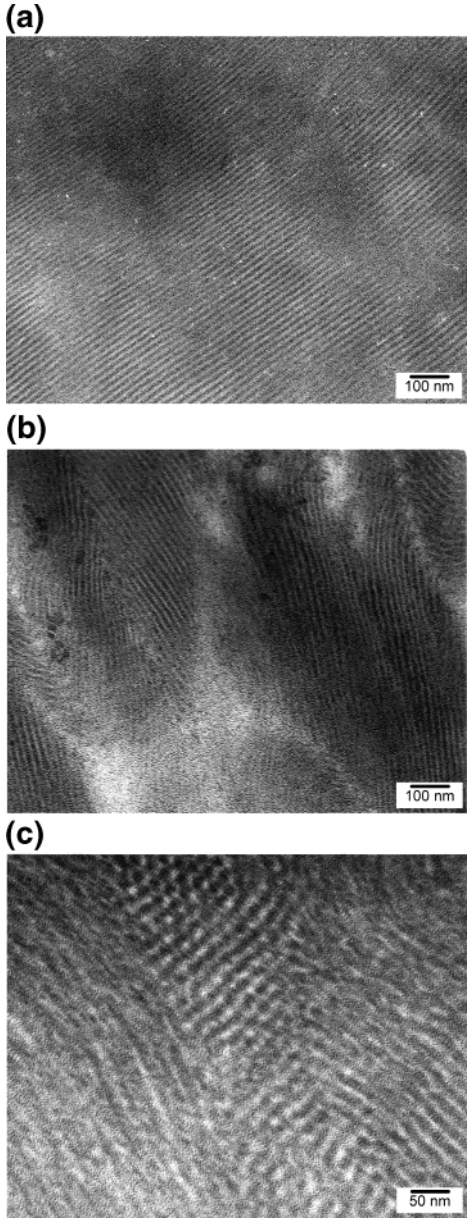

Figure 15. (a) TEM micrograph showing the lamellar morphology of sample A with 0.38 P*t*BVE volume fraction. (b) TEM micrograph showing the lamellar morphology of sample B with 0.32 P*t*BVE volume fraction. (c) TEM micrograph showing the cylindrical morphology of sample C with 0.22 P*t*BVE volume fraction.

which give domain spacings for samples A and B which are in agreement with the SAXS data rather than with the smaller spacings observed via TEM. Figure 16c shows the SAXS pattern of sample C, where there are four strong reflections with q_n/q^* ratios of 1, $\sqrt{3}$, 2, and $\sqrt{7}$, which are indicative of a cylindrical morphology. The d_{10} value calculated from SAXS is 28 nm, again larger than the TEM value, but in agreement with AFM results.

Results from AFM experiments on unannealed thin films of the triblock copolymers showed poorly ordered lamellar morphologies for samples A and B and a poorly ordered cylindrical morphology for sample C, consistent with our morphological assignments on the basis of TEM and SAXS data. The poor ordering of the spin cast samples is due to the short spinning process during which the polymer chains did not have enough time to

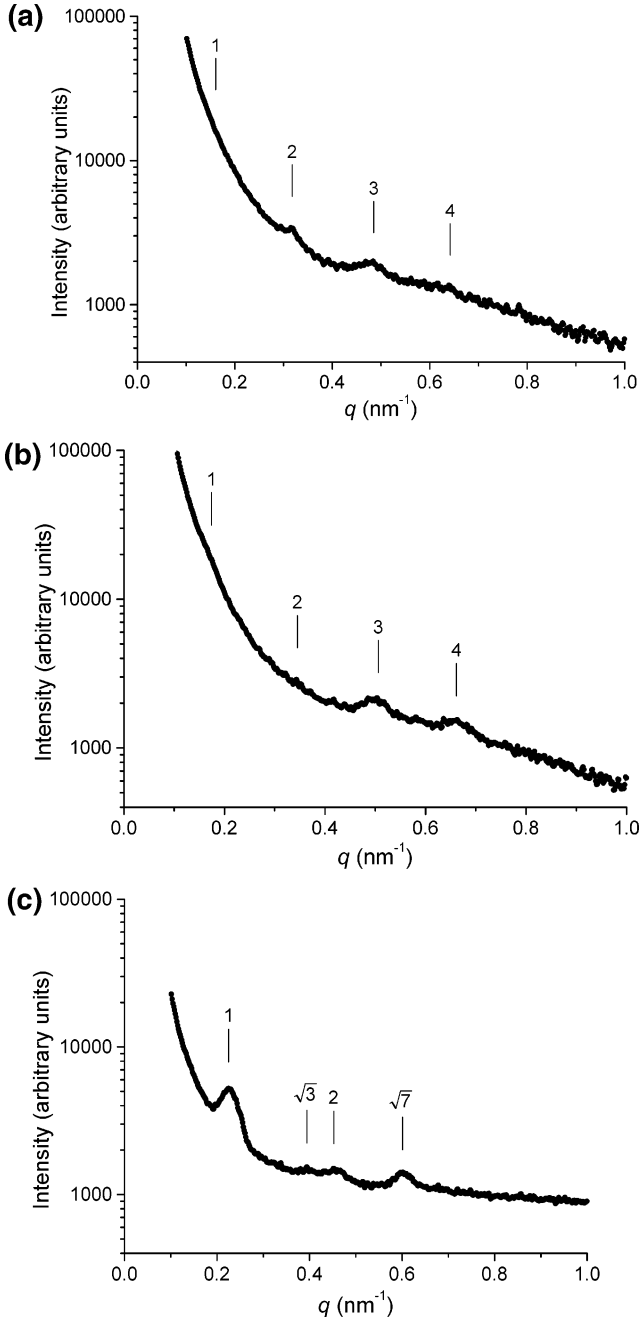

Figure 16. (a) SAXS pattern of sample A with 0.38 P*t*BVE volume fraction. (b) SAXS pattern of sample B with 0.32 P*t*BVE volume fraction. (c) SAXS pattern of sample C with 0.22 P*t*BVE volume fraction.

orient themselves to achieve good order. Nevertheless, the domain spacings measured from the AFM data on these unannealed films are good indicators of the domain spacings in the equilibrium state. The AFM values of the lamellar long periods for samples A and B are 44 and 41 nm, respectively, in agreement with SAXS data. The AFM value of d_{10} for sample C is 30 nm, also in agreement with SAXS data.

Conclusions

Efficient block copolymerization of IB with *t*BVE can be accomplished by living cationic polymerization in a one-pot capping-tuning process, which involves capping the living PIB chain ends with DTE followed by tuning the Lewis acidity by the addition of $Ti(OIp)_4$. The Lewis acidity, governed by the $[Ti(OIp)_4]/[TiCl_4]$ ratio, is critical for successful block copolymerization. Although 100% crossover efficiency could be achieved with all studied $[Ti(OIp)_4]/[TiCl_4]$ ratios, high Lewis acidity (low ratio) leads to too rapid polymerization and poor control over MWD, and low Lewis acidity (high ratio) resulted in undesirably slow polymerization. Using an optimum $[Ti(OIp)_4]/[TiCl_4]$ ratio well-defined PIB-P*t*BVE diblock and P*t*BVE-PIB-P*t*BVE triblock copolymers with designed molecular weight and narrow MWDs could be prepared, virtually without homopolymer contaminants. The triblock copolymers exhibited typical TPE properties with tensile strengths of 9−15 MPa and ultimate elongations of 760−1300%. TEM, SAXS, and AFM results suggested that samples with P*t*BVE volume fractions of 0.38 and 0.32 yield lamellar morphologies, and the sample with 0.22 P*t*BVE volume fraction exhibits cylindrical morphology.

Acknowledgment. Financial support from Boston Scientific Corp. is gratefully acknowledged.

References and Notes

(1) Miyamoto, M.; Sawamoto, M.; Higashimura, T. *Macromolecules* **1984**, *17*, 265−268.
(2) Faust, R.; Kennedy, J. P. *Polym. Bull.* **1986**, *15*, 317−323.
(3) Kennedy, J. P.; Iván, B. *Designed Polymers by Carbocationic Macromolecular Engineering: Theory and Practice*; Hanser Publishers: Munich, Germany, 1992.
(4) Matyjaszewski, K., Ed. *Cationic Polymerizations, Mechanisms, Synthesis and Application*; Marcel Dekker: New York, 1996.
(5) Puskas, J. E.; Kaszas, G. *Prog. Polym. Sci.* **2000**, *25*, 403−452.
(6) (a) Kaszas, G.; Puskas, J. E.; Kennedy, J. P.; Hager, W. G. *J. Polym. Sci., Part A: Polym. Chem.* **1991**, *29*, 427−435. (b) Storey, R. F.; Chisholm, B. J. *Macromolecules* **1993**, *26*, 6727−6733. (c) Gyor, M.; Fodor, Zs.; Wang, H.-C.; Faust, R. *J. Macromol. Sci.* **1994**, *A31* (12), 2055−2065.
(7) Kennedy, J. P.; Midha, S.; Tsunogal, Y. *Macromolecules* **1993**, *26*, 429−435.
(8) Fodor, Z.; Faust, R. *J. Macromol. Sci., Pure Appl. Chem.* **1995**, *A32* (3), 575−591.
(9) Li, D.; Faust, R. *Macromolecules* **1995**, *28*, 4893−4898.
(10) Sipos, L.; Zsuga, M.; Deák, G. *Macromol. Rapid Commun.* **1995**, *16*, 935−940.
(11) Kwon, Y.; Faust, R. *Macromolecules* **2002**, *35*, 3348−3357.
(12) Kim, M. S.; Faust, R. *Polym. Bull.* **2002**, *48*, 127−134.
(13) Coca, S.; Matyjaszewski, K. *J. Polymer. Sci.. Part A: Polym. Chem.* **1997**, *35*, 3595−3601.
(14) Feldthusen, J.; Iván, B.; Müller, A. H. E. *Macromolecules* **1998**, *31*, 578−585.
(15) Bae, Y. C.; Hadjikyriacou, S.; Schlaad, H.; Faust, R. In *Ionic Polymerization and Related Processes*; Puskas J. E., Ed.; Kluwer Academic Publishers: Dordrecht, Germany, 1999.
(16) Lubnin, A. V.; Kennedy, J. P. *J. Polym. Sci., Part A: Polym. Chem.* **1993**, *31*, 2825−2834.
(17) Kurian, J. Ph.D. Thesis, The University of Akron, 1991.
(18) Fodor, Z.; Faust, R. *J. Macromol. Sci., Pure Appl. Chem.* **1994**, *A31* (12), 1985−2000.
(19) Hadjikyriacou, S.; Faust, R. *Macromolecules* **1996**, *29*, 5261−5267.
(20) Hadjikyriacou, S.; Faust, R. *Macromolecules* **1995**, *28*, 7893−7900.
(21) Li, D.; Faust, R. *Macromolecules* **1995**, *28*, 1383−1389.
(22) Fishbein, L.; Crowe, B. F. *Makromol. Chem.* **1961**, *48*, 221−228.
(23) Okamura, S.; Kodama, T.; Higashimura, T. *Makromol. Chem.* **1962**, *53*, 180−191.
(24) Ohgi, H.; Sato, T. *Macromolecules* **1999**, *32*, 2403−2409.
(25) Aoshima, S.; Iwasa, S.; Kobayashi, E. *Polym. J.* **1994**, *26* (8), 912−919.
(26) Roth, M.; Mayr, H. *Macromolecules* **1996**, *29*, 6104−6109.
(27) Györ, M.; Wang, H.-C.; Faust, R. *J. Macromol. Sci., Pure Appl. Chem.* **1992**, *A29*, 639−653.
(28) Bae, Y. C.; Faust, R. *Macromolecules* **1998**, *31*, 2480−2487.
(29) Ledwith, A.; Lockett, E.; Sherrington, D. C. *Polymer* **1975**, *16*, 31−37.

(30) Pernecker, T.; Kennedy, J. P.; Ivan, B. *Macromolecules* **1992**, *25*, 1642−1647.
(31) Schlaad, H.; Kwon, Y.; Faust, R.; Mayr, H. *Macromolecules* **2000**, *33*, 743−747.
(32) Schlaad, H.; Kwon, Y.; Faust, R.; Charleux, B. *Macromolecules* **2000**, *33*, 8225−8232.
(33) Zhou, Y.; Faust, R. *Polymer Prepr.* **2003**, *44* (2), 661−662.
(34) Hatada, K.; Kitayama, T.; Matsuo, N.; Yuki, H. *Polym. J.* **1983**, *15* (10), 719−725.
(35) Kawaguchi T.; Sanda, F.; Masuda, T. *J. Polymer. Sci., Part A: Polym. Chem.* **2002**, *40*(22), 3938−3943.
(36) Ouchi, M.; Kamigaito, M.; Sawamoto, M. *Macromolecules* **1999**, *32*, 6407−6411.
(37) Brandrup, J., Immergut, E. H., Grulke, E. A., Bloch, D., Eds. *Polymer Handbook*, 4th ed.; John Wiley & Sons: New York, 1999.
(38) Trent, J. S.; Scheinbeim, J. I.; Couchman, P. R. *Macromolecules* **1983**, *16*, 589−598.
(39) Gido, S. P.; Thomas, E. L. *Macromolecules* **1994**, *27*, 6137−6144.

MA049424U